Contribution from the Department of Chemistry, University of Virginia, Charlottesville, Virginia 22901

Optical Activity of Transition Metal Compounds. III. Molecular Orbital Calculations on Six-Coordinate Complexes of Trigonal Symmetry[1]

R. W. STRICKLAND and F. S. RICHARDSON*[2]

Received October 13, 1972

Rotatory strengths for the d-d transitions of trigonally distorted six-coordinate complexes of Co^{3+} and Cr^{3+} with N and O donor atoms are calculated on a molecular orbital model. The electronic states of spectroscopic interest are constructed from molecular orbitals calculated on a modified Wolfsberg-Helmholz model. Calculations are carried out on ML_6 (M = metal atom, L = donor or ligator atom) clusters in which either the nuclear geometry of ML_6 has D_3 point group symmetry or the ligator donor orbitals are trigonally disposed about the metal atom. That is, chirality is introduced into the ML_6 cluster either by a Piper representation (trigonal nuclear geometry) or by a Liehr representation (ligand donor orbitals canted from the M-L axes in an octahedral ML_6 cluster). Additional calculations are carried out in which both a trigonally distorted ML_6 cluster and canted donor orbitals are present simultaneously. Rotatory strengths are calculated as functions of several stereochemical and electronic structural variables which are related to the chirality of D_3 complexes. The results suggest that neither the Piper molecular orbital model nor the Liehr model provides an adequate representation of the source of d-d optical activity in trigonal dihedral metal complexes. These molecular orbital models do, however, provide a means of deducing qualitative information about the sensitivity of d-d rotatory strengths to distortions within the ML_6 cluster.

I. Introduction

Transition metal complexes of trigonal dihedral (D_3) symmetry have played a prominent role as model systems in both experimental and theoretical investigations of natural optical activity. The first purely theoretical examination of the origin of optical activity in tris(bidentate ligand)metal complexes was made by Kuhn and Bein.[3-5] Their treatment of these systems was based on the general coupled-oscillator model of molecular optical activity proposed by Kuhn.[6-8] Selecting the tris complexes $Co(en)_3^{3+}$ and $Co(ox)_3^{3-}$ as model systems, Kuhn and Bein postulated that electronic transitions localized on the metal ion gained optical activity by coupling with electric dipole oscillators localized on the three bidentate ligands. More specifically, they represented the optical electron on the metal ion as an isotropic harmonic oscillator with a given frequency (say, ν_M) and the ligands by three linear oscillators of frequency ν_L ($\nu_L > \nu_M$) directed along the edges of the octahedron spanned by the chelate rings. On this model, the spatial arrangement of the three ligand oscillators is dissymmetric and their *coupled* motions give rise to a dissymmetric force field. If the metal ion oscillator is, in turn, coupled to the ligand oscillators *via* this dissymmetric force field, then optical activity will be observed at the frequencies of the perturbed metal oscillator (*i.e.*, in the metal ion absorption bands near ν_M), as well as at the frequencies of the perturbed ligand oscillators (*i.e.*, in the ligand absorption bands near ν_L).

The limitations and shortcomings of Kuhn's coupled-oscillator model, applied to the optical activity of d-d transitions in metal complexes, have been discussed in some detail elsewhere[9-12] and need not be rediscovered here. Recently, Mason, Bosnich, Hawkins, and Ferguson and their coworkers have developed the quantum mechanical analog to Kuhn's classical coupled-oscillator model and have applied this theory with considerable success to the circular dichroism (CD) spectra associated with the ligand-ligand transitions in tris and bis complexes of bidentate ligands which have moderately intense absorption bands in the near-ultraviolet spectrum.[13-23] However, Kuhn's coupled-oscillator model has, for the most part, been abandoned in current treatments of the optical activity manifested by the d-d and metal-ligand charge-transfer transitions in metal complexes.

Moffitt[24] introduced the first quantum mechanical theory of optical activity in chiral transition metal complexes. He adopted a crystal field model on which to represent the spectroscopic states of the metal ion d electrons and used the "one-electron" theory of optical activity proposed by Condon, Altar, and Eyring[25] to develop expressions for the rotatory strengths of the metal d-d transitions. An error in sign in the d-d transition matrix of the angular momentum operator led Moffitt to incorrect conclusions, and Sugano[26] subsequently demonstrated that Moffitt's model could not account for the net optical activity observed for the $^1A_{1g} \rightarrow {}^1T_{1g}$ transition in trigonal dihedral complexes of Co(III) and for the $^4A_{2g} \rightarrow {}^4T_{2g}$ transition in Cr(III) complexes of

(1) (a) Part I: F. S. Richardson, *J. Chem. Phys.*, 54, 2453 (1971); part II: F. S. Richardson, *ibid.*, 57, 589 (1972). (b) This work was supported by a grant from the Petroleum Research Fund, administered by the American Chemical Society.

(2) Fellow of the Camille and Henry Dreyfus Foundation.

(3) W. Kuhn and K. Bein, *Z. Phys. Chem., Abt. B*, 24, 335 (1934).

(4) W. Kuhn and K. Bein, *Z. Anorg. Allg. Chem.*, 216, 321 (1934).

(5) W. Kuhn, *Naturwissenschaften*, 19, 289 (1938).

(6) W. Kuhn, *Z. Phys. Chem., Abt. B*, 4, 14 (1929).

(7) W. Kuhn, *Trans. Faraday Soc.*, 26, 293 (1930).

(8) W. Kuhn, *Z. Phys. Chem., Abt. B*, 20, 325 (1933).

(9) C. J. Hawkins, "Absolute Configuration of Metal Complexes," Wiley-Interscience, New York, N. Y., 1971, Chapter 5.

(10) F. Woldbye, *Rec. Chem. Progr.*, 24, 197 (1963).

(11) S. F. Mason, *Quart. Rev., Chem. Soc.*, 17, 20 (1963).

(12) A. J. McCaffery and S. F. Mason, *Mol. Phys.*, 6, 359 (1963).

(13) B. Bosnich, *Accounts Chem. Res.*, 2, 266 (1969).

(14) E. Larsen, S. F. Mason, and G. H. Searle, *Acta Chem. Scand.*, 20, 191 (1966).

(15) A. J. McCaffery and S. F. Mason, *Proc. Chem. Soc., London*, 211 (1963).

(16) J. Mason and S. F. Mason, *Tetrahedron*, 23, 1919 (1967).

(17) S. F. Mason, *Inorg. Chim. Acta Rev.*, 2, 89 (1968).

(18) B. Bosnich, *J. Amer. Chem. Soc.*, 90, 627 (1968).

(19) B. Bosnich, *Inorg. Chem.*, 7, 178, 2379 (1968).

(20) B. Bosnich and A. T. Phillip, *J. Amer. Chem. Soc.*, 90, 6352 (1968).

(21) R. G. Bray, J. Ferguson, and C. J. Hawkins, *Aust. J. Chem.*, 22, 2091 (1969).

(22) J. C. Ferguson, C. J. Hawkins, N. A. P. Kane-Maquire, and H. Lip, *Inorg. Chem.*, 8, 771 (1969).

(23) S. F. Mason and B. J. Norman, *Chem. Phys. Lett.*, 2, 22 (1968).

(24) W. Moffitt, *J. Chem. Phys.*, 25, 1189 (1956).

(25) E. U. Condon, W. Altar, and H. Eyring, *J. Chem. Phys.*, 5, 753 (1937).

(26) S. Sugano, *J. Chem. Phys.*, 33, 1883 (1960).

trigonal dihedral symmetry. However, Moffitt's work provided an important stimulus for much of the subsequent theoretical effort given to this subject.[27-41]

The crystal field one-electron model (or "ionic" model) has served as the basis for several additional theoretical studies on the optical activity of d-d transitions in metal complexes.[27-29,36,38-41] When this perturbation model is developed to second-order in the dissymmetric parts of the crystal field potential, it is found that a net rotatory strength is associated with d-d transitions which are degenerate in the zeroth-order cubic representation,[36,38-41] in agreement with experimental observations. Furthermore, this model has provided the basis for a set of sector (or regional) rules which have proved to be of some value in relating the stereochemical variables of metal complexes to the signs and magnitudes of of CD bands.[39-42]

The crystal field one-electron model admits only static coupling between the ground state, static charge distributions located in the perturbing ligand environment, and a chromophoric electron localized on the metal ion. Recently, Mason[32] and Richardson[40] have employed a more general perturbation model for interpreting the optical activity of transition metal complexes. The model they adopted is basically identical with that developed by Tinoco[43] in 1962 and, more recently, applied to organic systems by Hohn and Weigang.[44] It can be characterized as an independent-systems model insofar as the metal complex is partitioned into a number of separate groups (metal ion and ligand groups) and it is assumed that the electronic distributions of the individual groups do not overlap. To zeroth-order, it is further assumed that the electronic properties of each group can be approximated by considering the group to be isolated from the rest of the system. Interactions between groups are then treated by perturbation theory. It should be obvious that the crystal field one-electron model is subsumed by this general perturbation model. Both "one-electron" and "two-electron" terms arise in the general theory. The "one-electron" terms are so called because they involve the dynamic behavior of only one electron; the remaining charges in the system are assumed to provide an average or static field in which the "one-electron" must move. The "two-electron" terms originate with the coupled motions of two electrons, each localized in a separate group. For the d-d transitions of chiral metal complexes, the pairwise dynamic couplings between electrons in the ligand environment and the chromophoric d electron can provide significant contributions to the total d-d rotatory strength.[32,40,45]

Schaffer[37] has applied the angular overlap model[46] to the ligand field transitions of dissymmetric tris-bidentate and cis bis-bidentate complexes of d^3 and low-spin d^6 metal ions. Although this approach appears to have considerable merit for representing the essential aspects of the optical activity problem, a detailed account of its applications has not yet been given.

The first theoretical studies of optical activity in metal complexes to employ a molecular orbital representation of the spectroscopic states were reported by Liehr[34,35] and by Karipedes and Piper.[30] In the latter study, the molecular orbitals were constructed in the LCAO approximation, the ligand orbital basis set was restricted to the 2s and $2p\sigma$ atomic orbitals on the six ligator (donor) atoms, and the 3d and 4p orbitals of the metal ion were included. Metal-ligand π bonding was neglected. On this molecular orbital model, optical activity is generated by a trigonal distortion of the ML_6 σ-bonded structure; that is, the ligating atoms are displaced from the vertices of a regular octahedron and the resultant ML_6 cluster has trigonal dihedral (D_3) symmetry.

Distortions of ML_6 from an octahedral to a trigonal geometry may be characterized in terms of the polar angles θ_L and azimuthal angles ϕ_L of each ligator atom as measured with respect to a trigonal coordinate system centered on M (with the Z axis coincident with the C_3 axis of the distorted ML_6 cluster).[39] For tris-bidentate complexes in which the two ligator atoms of a single ligand are designated L and L′ (but are chemically identical), trigonal distortions are conveniently expressed in terms of azimuthal twists about the C_3 axis and polar elongation (or compression) of the complex along the C_3 axis. For an octahedral arrangement of the ML_6 cluster, the dihedral angle, $\omega = \phi_L - \phi_{L'}$, between each pair of donor atoms, L and L′, in the chelate system is 60°. Azimuthal twist operations lead to values of $\omega \neq 60°$. The four kinds of trigonal distortions involving both polar elongation (or compression) and azimuthal twist operations are listed as follows: (1) polar elongation-azimuthal expansion ($\omega > 60°$), (2) polar compression-azimuthal contraction ($\omega < 60°$), (3) polar elongation-azimuthal contraction, and (4) polar compression-azimuthal expansion. These distortions of the ML_6 cluster in tris(symmetric bidentate ligand) complexes are depicted in Figure 1. The tris(oxalate) and tris(ethylenediamine) complexes of Co(III) are examples of systems in which the ML_6 cluster suffers polar compression-azimuthal contraction (at least in crystalline media).[47-50] The tris(malonate) complex of Cr(III) in crystalline form reveals a polar elongation-azimuthal expansion of the CrO_6 cluster.[51] In $Co(ox)_3^{3-}$, $\omega = 54.0°$; in $Cr(mal)_3^{3-}$, $\omega = 60.6°$.[51] The tris(trimethylenediamine) complex of Co(III) also suffers polar elongation-azimuthal expansion in its crystalline

(27) N. K. Hamer, *Mol. Phys.*, 5, 339 (1962).
(28) H. Poulet, *J. Chim. Phys.*, 59, 584 (1962).
(29) T. S. Piper and A. Karipedes, *Mol. Phys.*, 5, 475 (1962).
(30) A. Karipedes and T. S. Piper, *J. Chem. Phys.*, 40, 674 (1964).
(31) A. J. McCaffery and S. F. Mason, *Mol. Phys.*, 6, 359 (1963).
(32) S. F. Mason, *J. Chem. Soc. A*, 667 (1971).
(33) Th. Burer, *Mol. Phys.*, 6, 541 (1963).
(34) A. Liehr, *J. Phys. Chem.*, 68, 665 (1964).
(35) A. Liehr, *J. Phys. Chem.*, 68, 3629 (1964).
(36) M. Shinada, *J. Phys. Soc. Jap.*, 19, 1607 (1964).
(37) C. E. Schaffer, *Proc. Roy. Soc., Ser. A*, 297, 96 (1968).
(38) D. J. Caldwell, *J. Phys. Chem.*, 71, 1907 (1967).
(39) F. S. Richardson, *J. Phys. Chem.*, 75, 692 (1971).
(40) F. S. Richardson, *J. Chem. Phys.*, 54, 2453 (1971); 57, 589 (1972).
(41) F. S. Richardson, *Inorg. Chem.*, 10, 2121 (1971); 11, 2366 (1972).
(42) B. Bosnich and J. Harrowfield, *J. Amer. Chem. Soc.*, 94, 3425 (1972).
(43) I. Tinoco, *Advan. Chem. Phys.*, 4, 67 (1962).
(44) E. G. Hohn and O. E. Weigang, *J. Chem. Phys.*, 48, 1127 (1968).
(45) P. L. Fereday and S. F. Mason, *Chem. Commun.*, 1314 (1971).
(46) C. E. Schaffer, *Struct. Bonding (Berlin)*, 5, 68 (1968).
(47) X-Ray structure analysis of the tris(oxalato)cobaltate(III) complex anion: K. R. Butler and M. R. Snow, *J. Chem. Soc. A*, 565 (1971).
(48) Y. Saito, K. Nakatsu, M. Shiro, and H. Kuroya, *Bull. Chem. Soc. Jap.*, 30, 795 (1957).
(49) K. Nakatsu, *Bull. Chem. Soc. Jap.*, 35, 832 (1962).
(50) M. Iwata, K. Nakatsu, and Y. Saito, *Acta Crystallogr., Sect. B*, 25, 2562 (1969).
(51) K. R. Butler and M. R. Snow, *Chem. Commun.*, 550 (1971).

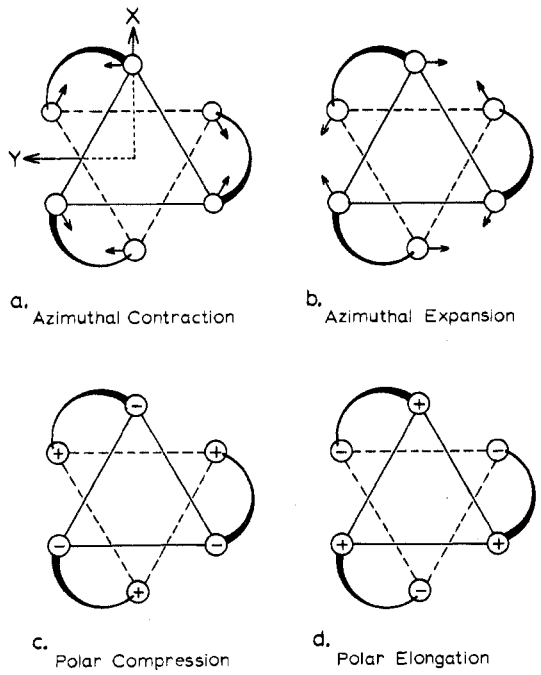

Figure 1. Trigonal distortion operations on the ML_6 cluster of a tris(bidentate ligand)metal complex with D(Λ) absolute configuration.

form.[52] However, Butler and Snow[53] have suggested that, in solution, $Co(tn)_3^{3+}$ may exist in forms in which the angles ω are contracted from 60° and the complex is compressed along the trigonal axis. The various structural forms of $Co(tn)_3^{3+}$ are attributed to the several possible conformations which each six-membered chelate ring may adopt.

A salient feature of the molecular orbital model presented by Karipedes and Piper[30] is that the net rotatory strength associated with the lowest lying cubic transition in tris-bidentate Cr(III) and tris-bidentate Co(III) complexes changes sign as the dihedral angle ω changes from less than 60° to greater than 60°. Since the chiral distribution of the chelate rings about the C_3 axis is neglected on this model, no optical activity, of course, is predicted for $\omega = 60°$. On this model, it is predicted that the net rotatory strengths will be of opposite sign for two complexes which have identical absolute configurations with respect to their chelate ring distributions but which suffer azimuthal twist distortions of opposite senses (*i.e.*, $\omega < 60°$ for one and $\omega > 60°$ for the other) in the ML_6 cluster. For example, the sign of the net CD observed for the $^1A_{1g} \rightarrow {}^1T_{1g}$ transition of tris-bidentate Co(III) complexes depends upon whether ω is greater than or less than 60° rather than upon the absolute configuration of the three bidentate ligands about the Co(III) ion. To calculate the correct sign for the net rotatory strength of Λ(+)-$Co(en)_3^{3+}$, Karipedes and Piper had to assume an expansion of the N-Co-N bond angle from 90° and a twist angle $\omega > 60°$. In the crystal, ∠N-Co-N = 85.3° and $\omega = 54.9°$ for Λ(+)-$Co(en)_3^{3+}$.[50] Although these results suggest that the Piper model yields incorrect absolute signs for the net rotatory strength, several recent studies on other systems tend to support the validity and qualitative accuracy of its predictions.[53,54]

Liehr constructed molecular orbital models for the optical activity of both six-coordinate complexes of trigonal dihedral symmetry[34] and four-coordinate complexes of digonal dihedral symmetry.[35] The essential feature of Liehr's model is a significant angle of "mis-match" between the directions of maximum charge density for the metal d orbitals and the donor orbitals of the ligating atoms. In the trigonal dihedral systems, the ligating atoms are situated at their octahedral positions but the ligator atom σ orbitals are canted with respect to the metal-ligator internuclear axis. This angle of cant (denoted as α) is sensitive to the detailed structural features of the chelate rings and all dissymmetry in the complex is communicated to the metal ion *via* this deviation of each primary metal-ligator linkage from axial symmetry (about the M-L direction). In this treatment the rotatory strength turns out to be proportional to $\sin \alpha$.

Liehr did not carry out detailed computations based on his model and the conceptual basis of the model is not easily transformed into working hypotheses which can be tested by experiment. Piper and Karipedes[55] calculated the dipole strengths of the $Cu(en)_3^{3+}$ system using Liehr's bent-bond model and concluded that it underestimates the electric dipole transition integrals by at least an order of magnitude. However, it is a fair statement that Liehr's model has not yet been adequately tested.

Most of the experimental CD data obtained on the d-d transitions of metal complexes with trigonal dihedral symmetry presently are interpreted in terms of Piper's molecular orbital model, Mason's semiempirical method for relating the sign of the doubly degenerate long-wavelength transition to absolute configuration, or the sector (regional) rules developed on the basis of the one-electron static coupling and two-electron dynamical coupling models. Presumably, Piper's model is useful for relating the spectroscopic observables to distortions within the ML_6 cluster, and the sector rules are applicable for obtaining information about stereochemical features of the ligand environment beyond the ML_6 cluster. For most systems, it is quite probable that both ML_6 distortions and the nonligating parts of the ligand environment will contribute to the net optical activity of the complex. Unfortunately, a unified theory in which these contributions are treated simultaneously does not exist. The independent-systems theory, which includes both the one-electron static coupling model and the two-electron dynamical coupling model, cannot deal appropriately with atoms attached directly to the chromophoric site (the metal ion), and a molecular orbital model which encompasses the entire complex is unsuitable from a computational quantum chemical point of view.

The primary purpose of the present study was to refine and extend Piper's molecular orbital model so that the current controversies provoked by the predictions of his model could be placed in sharper focus. Although our computational methods are somewhat more refined than those of Karipedes and Piper and we extend the calculations to include a larger number of structural variables (*e.g.*, π bonding, various donor atoms and metal ions, etc.), our computational model is too crude to permit more than qualitative or semiquantitative conclusions. For purposes of comparison we also carried out several calculations based essentially on Liehr's model. That is, we allowed for displacement of the ligands from the octahedral axes and for canting of the ligand p_σ orbital with respect to the metal-ligand bond axes. In real systems these two types of distortion can occur simultaneously.

(52) T. Nomura, F. Marumo, and Y. Saito, *Bull. Chem. Soc. Jap.*, 42, 1016 (1969).
(53) K. Butler and M. Snow, *Inorg. Chem.*, 10, 1338 (1971).
(54) R. M. Wing and R. Eiss, *J. Amer. Chem. Soc.*, **92**, 1929 (1970).
(55) T. S. Piper and A. G. Karipedes, *Inorg. Chem.*, **4**, 923 (1965).

II. Model

A. Molecular Orbital Calculation. 1. General Procedure. We assume a six-coordinate metal complex in which six identical ligand atoms are coordinated to a central transition metal ion. We adopt an octahedral reference geometry for the ML_6 cluster and describe all other geometries of ML_6 in terms of distortions from this O_h reference configuration. In this study we are, of course, principally interested in the trigonally distorted forms of ML_6 which have exact trigonal dihedral (D_3) symmetry. For this reason, it is convenient to express the positions of the ligand atoms in terms of a trigonal coordinate system with its origin at the metal atom and one of its axes coincident with a C_3 axis of the ML_6 octahedron. With respect to the cubic coordinate system (X_o, Y_o, Z_o) shown in Figure 2, the Z axis of the trigonal coordinate system (X, Y, Z) points along the (111) direction and the X axis is in the plane formed by a ligand-metal axis and the Z axis. Specification of (X, Y, Z) as a right-handed, orthogonal coordinate system fixes Y.

Trigonal distortions of the ML_6 cluster from regular octahedral symmetry are expressed in terms of two angular variables: σ = distortion angle measuring polar compression ($\sigma < 0$) or polar elongation ($\sigma > 0°$) of the ML_6 cluster along the C_3 (Z) axis; δ = distortion angle measuring azimuthal twist about the C_3 (Z) axis (see Figure 3). For a twist operation in which the upper triad of ligand atoms in Figure 3 is rotated counterclockwise (CCW) about the C_3 axis (viewed from the positive Z direction) and the lower triad is rotated clockwise (CW) by the same amount, $\delta > 0°$. If the directions of rotation of the two triads are reversed, then $\delta < 0°$. A trigonal twist operation of either sense ($\delta > 0°$ or $\delta < 0°$) results in a total change in dihedral angle of $\Delta\omega = |2\delta|$ for each of the ligand pairs, (1,1′), (2,2′), and (3,3′). In a polar elongation of ML_6, the polar angles of ligands 1, 2, and 3 are less than the octahedral value of 54.74° (*i.e.*, $\theta_L < 54.74°$), and the polar angles of ligands 1′, 2′, and 3′ are greater than the octahedral value of 125.26° (*i.e.*, $\theta_L' > 125.26°$). For a polar compression, $\theta_L > 54.74°$ and $\theta_L' < 125.26°$.

In addition to the metal-centered coordinate system, six ligand-centered coordinate systems were required in order to define the ligand atomic orbitals. The localized ligand coordinate systems are shown in Figure 2. Note that the z axes of the localized ligand systems all point directly toward the metal atom. The metal-ligand σ bonds are defined to have cylindrical symmetry about these axes, in accordance with the earlier molecular orbital model of Karipedes and Piper[30] but differing from the model proposed by Liehr.[34]

Calculations on the model of Karipedes and Piper are made by deleting the ligand p_π atomic orbitals from the basis set. Canting of the ligand p_σ orbital, Liehr's model, is accomplished by expressing the canted orbital as a linear combination of the ligand p_x, p_y, and p_z orbitals. First the p_x and p_y orbitals are rotated counterclockwise (see Figure 2) about the metal-ligand internuclear axis through an angle λ. The angle of cant, α, is defined in the figure

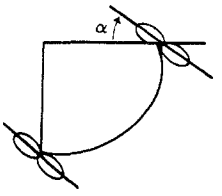

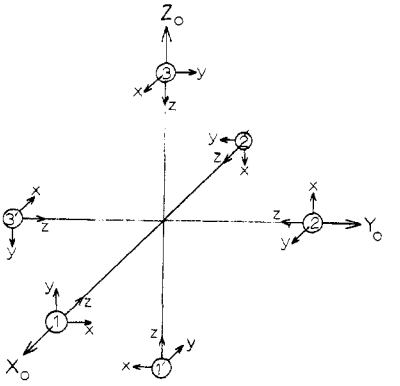

Figure 2. Cubic coordinate system (X_o, Y_o, Z_o) centered on the metal atom and the local ligand coordinate systems.

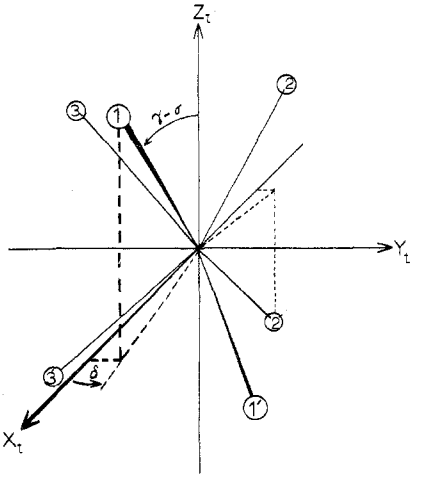

Figure 3. Definitions of distortion angles σ and δ. The trigonal coordinate system is denoted by (X_t, Y_t, Z_t) and the angle γ is 54.74°.

Having specified α, the canted p_σ orbital is given by

$$p_\sigma = p_z \cos\alpha + 2^{-1/2}(p_x' + p_y')\sin\alpha$$

where the primes on p_x and p_y denote rotation through λ. For a planar ligand in a complex with Λ configuration, $\lambda = 45°$. (For the Δ configuration, $\lambda = -45°$.) The flexibility of the model allows us to treat the so-called "lel" and "ob" isomers of $Co(en)_3^{3+}$.[9] For the Λ configuration the "lel" isomer would have $\lambda = 60°$, while for the "ob" isomer, $\lambda = 30°$.

The atomic orbital (AO) basis for the molecular orbital (MO) calculation consisted of the 4s, 4p, and double-ζ 3d metal orbitals and the 2s (or 3s) and 2p (or 3p) orbitals on each ligand atom. The 3d, 4s, and 4p basis orbitals on the metal ion, expressed in terms of both octahedral and trigonal coordinates, are listed in Table I along with the irreducible representations (IR) for which they form bases in the O_h and D_3 point groups. In Table II are listed the ligand symmetry orbitals, chosen to transform as bases for IR's in both O_h and D_3 and expressed in terms of the six localized ligand coordinate systems shown in Figure 2.

The molecular orbitals are obtained by use of a modified Wolfsberg-Helmholz[56] or extended Huckel[57] treatment. In this method we first solve the equation

$$\det(H_{ij} - \epsilon S_{ij}) = 0 \qquad (1)$$

(56) M. Wolfsberg and L. Helmholz, *J. Chem. Phys.*, **20**, 837 (1952).

(57) R. Hoffman, *J. Chem. Phys.*, **39**, 1397 (1963); **40**, 2474, 2480, 2745 (1964).

Table I. Central Ion Basis Functions in Octahedral and Trigonal Coordinates

Basis functions	Irreducible representations		Symmetry orbitals	
	O_h	D_3	Octahedral	Trigonal
$\phi_e^+(d)$	E_g	$E(\theta)$	$d_{z_O^2}$	$(1/3)^{1/2}[d_{x^2-y^2} + 2^{1/2}d_{xz}]$
$\phi_e^-(d)$	E_g	$E(\epsilon)$	$d_{x_O^2-y_O^2}$	$-(1/3)^{1/2}[d_{xy} - 2^{1/2}d_{yz}]$
$\phi_t^+(d)$	T_{2g}	$E(\rho)$	$(1/6)^{1/2}[2d_{x_Oy_O} - d_{y_Oz_O} - d_{x_Oz_O}]$	$(1/3)^{1/2}[2^{1/2}d_{x^2-y^2} - d_{xz}]$
$\phi_t^-(d)$	T_{2g}	$E(\sigma)$	$(1/2)^{1/2}[d_{y_Oz_O} - d_{x_Oz_O}]$	$-(1/3)^{1/2}[2^{1/2}d_{xy} + d_{yz}]$
$\phi_t^0(d)$	T_{2g}	$A_1(\tau)$	$(1/2)^{1/2}[d_{x_Oy_O} + d_{x_Oz_O}]$	d_{z^2}
$\phi_t^+(p)$	T_{1u}	$E(x)$	$(1/6)^{1/2}[2p_{z_O} - p_{x_O} - p_{y_O}]$	p_x
$\phi_t^-(p)$	T_{1u}	$E(y)$	$(1/2)^{1/2}[p_{x_O} - p_{y_O}]$	p_y
$\phi_t^0(p)$	T_{1u}	A_2	$(1/3)^{1/2}[p_{x_O} + p_{y_O} + p_{z_O}]$	p_z
$\phi_a(s)$	A_{1g}	A_1		

for the energies ϵ and then find the coefficients C_{mi} for the molecular orbitals

$$\psi_m = \sum_i^N C_{mi}\phi_i \tag{2}$$

where the ϕ_i are the atomic orbitals in our basis set.

The calculation proceeds as follows. First the overlap matrix is computed and diagonalized to obtain $\mathbf{S}^{-1/2}$. From input populations of the various orbitals, the free ion VOIP are computed according to the procedure formulated by Anno and Sakai.[58] Next the crystal field terms are added to the metal ion VOIP to obtain the metal diagonal elements of the Hamiltonian matrix.[59] The metal-metal part of the Hamiltonian matrix (**H**) is comprised entirely of crystal field (CF) terms. The negatives of the VOIP are used for the ligand diagonal elements of **H** and a Wolfsberg-Helmholz (W-H) procedure is employed in determining the ligand-ligand off-diagonal elements. The metal-ligand off-diagonal elements of **H** are also computed by a W-H procedure in which different parameters are used to distinguish between σ- and π-type interactions.

The eigenvalue equation to solve is $|\mathbf{H} - \epsilon\mathbf{S}| = 0$. In the ZDO approximation, the usual procedure is to find the inverse of **S** and operate on the eigenvalue equation to obtain $|\mathbf{S}^{-1}\mathbf{H} - \epsilon| = 0$. Then $\mathbf{S}^{-1}\mathbf{H}$ is diagonalized to obtain the eigenvalues and eigenvectors. However, except for special cases, $\mathbf{S}^{-1}\mathbf{H}$ is not symmetric and the usual diagonalization subroutines cannot be used. To circumvent this problem we first find $\mathbf{H}' = \mathbf{S}^{-1/2}\mathbf{H}\mathbf{S}^{-1/2}$ and then diagonalize $\mathbf{H}'$ to obtain $\epsilon = \mathbf{D}^{-1}[\mathbf{S}^{-1/2}\mathbf{H}\mathbf{S}^{-1/2}]\mathbf{D}$. The eigenvectors are then given by $\mathbf{C} = \mathbf{S}^{-1/2}\mathbf{D}$. Having obtained the eigenvectors we than compute orbital population by Mulliken's method.[60] From the normalization condition

$$1 = \langle\psi_m|\psi_m\rangle = \langle\sum_i C_{mi}\phi_i|\sum_j C_{mj}\phi_j\rangle = \sum_i C_{mi}\sum_j C_{mj}S_{ij} \tag{3}$$

The population of atomic orbital i is defined as $C_{mi}\Sigma_j C_{mj}S_{ij}$ for the mth molecular orbital. For N filled molecular orbitals, the population of atomic orbital i is given by $2\Sigma_{m=1}^{N} C_{mi}\Sigma_j C_{mj}S_{ij}$. If P_i' is the input population of orbital i and P_i'' is the output population, then we define an average population, $P_i = (1 - \lambda)P_i' + \lambda P_i''$, and use this value as input for the next recalculation of the Hamiltonian matrix. This procedure is done iteratively until self-consistency is achieved. The constant, λ, is introduced as a damping factor to avoid extreme oscillations in the calculations. When at least three iterations have been made, an extrapolation procedure[61] is used to approximate the self-consistant populations. After the kth iteration has taken place, the extrapolated population of the ith atomic orbital to be used in the $(k + 1)$th cycle is obtained from

$$P_i^{(k+1)} = P_i^{(k)} - T^{(k)}(\Delta_i^{(k)} + \delta_i^{(k)})/(T^{(k)} + W^{(k)}) \tag{4}$$

where

$$\Delta_i^{(k)} = (P_i^{(k)} - P_i^{(k-1)})^2/(P_i^{(k)} - 2P_i^{(k-1)} + P_i^{(k-2)})$$

$$W^{(k)} = \sum_j \Delta_j^{(k)}$$

$$T^{(k)} = \sum_j |\Delta_j^{(k)}|$$

$$\delta_i^{(k)} = -|\Delta_i^{(k)}|W^{(k)}/T^{(k)}$$

In performing the calculations we fixed the ligand VOIP at the free-ion values. Generally, self-consistency for the orbital populations is reached in six or seven iterations.

2. Overlap Matrix. We afix a minimum valence basis set of Slater-type atomic orbitals (STO) to each ligand such that the local Z axis on each ligand points toward the metal ion. The atomic orbitals on the metal ion are quantized about the C_3 axis which is collinear with the reference coordinate Z axis. The overlap integrals between metal and ligand orbitals are computed from formulas given by Lofthus[62] while ligand-ligand overlaps are calculated from formulas due to Mulliken, *et al.*[63] In both cases we calculate the overlaps for a "local diatomic" system at the appropriate distance and project them onto the molecular system. The latter is accomplished by means of a unitary transformation matrix derived from the Euler angles relating the molecular system to the "local diatomic" system.

3. Hamiltonian Matrix. The diagonal terms of the Hamiltonian matrix may be shown[59] to have the form

$$H_{ii} = -\mathrm{VOIP}(i) + V_{\mathrm{CF}}^{(i)} \tag{5}$$

where $V_{\mathrm{CF}}^{(i)}$ is the crystal field potential arising from the molecular core screened by its ground state distribution of valence electrons. The appropriate VOIP for a given orbital depends upon the ground-state populations of all valence orbitals located on the same nucleus.

We partition the trigonal (D_3) crystal field potential into gerade and ungerade parts

$$V_{\mathrm{CF}} = V_g + V_u \tag{6}$$

where

(58) T. Anno and Y. Sakai, *J. Chem. Phys.*, **56**, 922 (1972).
(59) R. F. Fenske, K. G. Caulton, D. D. Radtke, and C. C. Sweeney, *Inorg. Chem.*, **5**, 951 (1966).
(60) R. S. Mulliken, *J. Chem. Phys.*, **23**, 1833 (1955).
(61) W. Yeakel, Ph.D. Dissertation, University of Wisconsin, 1972.
(62) A. Lofthus, *Mol. Phys.*, **5**, 105 (1962).
(63) R. S. Mulliken, C. A. Rieke, D. Orloff, and H. Orloff, *J. Chem. Phys.*, **17**, 1248 (1949).

$$V_u = -[5\pi/4]^{1/2}(Y_3^{-3} - Y_3^{3})r^3 \sum_{L=1}^{6} Q_L R_L^{-4} \times \sin^3 \theta_L \cos 3\phi_L \quad (7)$$

and

$$V_g = -r^2 Y_2^0 \sum_{L=1}^{6} Q_L[6R_L^{-1} + 3R_L^{-3}(4\pi/5)^{1/2}(3\cos^2 \theta_L - 1)] - r^4 Y_4^0(\pi/4)^{1/2}\sum_L Q_L R_L^{-2}(35\cos^4 \theta_L - 30\cos^2 \theta_L + 3) - r^4(Y_4^{-3} - Y_4^{3})(35\pi)^{1/2}\sum_L Q_L R_L^{-4} \times \sin^3 \theta_L \cos \theta_L \quad (8)$$

where the spherical harmonic functions Y_l^m depend upon electron coordinates and are centered on the metal atom, θ_L and ϕ_L refer to ligand positions as shown in Figure 2, and Q_L is the charge on ligand L. Formulas for the nonzero CF matrix elements are given in Table III.

The diagonal ligand CF matrix elements are computed as

$$V_{CF}(\text{ligand L}) = -Q_M R_L^{-1} - Q_L \sum_{L' \neq L} R_{L,L'}^{-1} \quad (9)$$

where Q_M is the ground-state charge on the metal. In deriving this expression we have neglected the spatial extent of the ligand orbitals. However, since our principal interest lies predominantly with metal-metal transitions, this neglect should have little effect on our results.

The off-diagonal H matrix elements between metal orbitals consist entirely of crystal field terms. By symmetry V_u will mix 3d and 4s orbitals with 4p orbitals, while V_g will mix the 3d and 4p orbitals among themselves. The nontrivial matrix elements are given in Table III. In evaluating the CF matrix elements we require values for the radial terms: $\langle R_{3d}|r^2|R_{3d}\rangle$, $\langle R_{3d}|r^4|R_{3d}\rangle$, $\langle R_{3d}|r^2|R_{4s}\rangle$, $\langle R_{3d}|r^3|R_{4p}\rangle$, and $\langle R_{4p}|r^2|R_{4p}\rangle$. These are calculated by means of the formulas in Table IV. Here R_k is the normalized radial portion of the atomic orbital of type k.

We choose to calculate the metal-ligand and ligand-ligand off-diagonal H matrix elements by a modified Wolfsberg-Helmholz procedure. The general expression for these matrix elements is

$$H_{ij} = FS_{ij}(\text{VOIP}_i + \text{VOIP}_j)/2 \quad (10)$$

where F is a parameter which may assume different values depending on whether the overlap is ligand-ligand, ligand-metal σ type, or ligand-metal π type. In our calculations we use F values reported by Basch, Viste, and Gray.[64] We take the arithmetic mean of the VOIP rather than the diagonal matrix elements since the latter contain crystal field terms. Berthier, *et al.*,[65] have shown that when the Wolfsberg-Helmholz procedure is used, an adjustment must be made for a change in the zero point of energy. This adjustment is avoided by using VOIP since the values of F that we use were optimized in calculations using VOIP as the diagonal elements of the H matrix.

B. Excited States. The virtual orbital approximation is used in constructing the excited states. For m filled MO's in the ground state, the ground-state wave function is taken to be the Slater determinant

$$\Psi_0 = |\psi_1(1)\bar{\psi}_1(2)\psi_2(3)\ldots\bar{\psi}_m(2m)| \quad (11)$$

where a bar denotes an electron with β spin and the absence of a bar denotes α spin. The Slater determinant corresponding to the excitation of an electron from the kth to

(64) H. Basch, A. Viste, and H. B. Gray, *J. Chem. Phys.*, 44, 10 (1966).
(65) G. Berthier, G. Del Re, and A. Veillard, *Nuovo Cimento B*, 44, 315 (1966).

Table II. Ligand Symmetry Orbitals Expressed in Terms of Local Ligand Coordinate Systems

Symmetry orbitals	Irreducible representations O_h	Irreducible representations D_3	Linear combinations of ligand AO's[a]
χ_1	A_{1g}	A_1	$(1/6)^{1/2}(Z_1 + Z_2 + Z_3 + Z_1' + Z_2' + Z_3')$
χ_2	A_{1g}	A_1	$(1/6)^{1/2}(S_1 + S_2 + S_3 + S_1' + S_2' + S_3')$
χ_3	E_g	$E(\theta)$	$-(1/12)^{1/2}(Z_1 + Z_2 - 2Z_3 + Z_1' + Z_2' - 2Z_3')$
χ_4	E_g	$E(\theta)$	$-(1/12)^{1/2}(S_1 + S_2 - 2S_3 + S_1' + S_2' - 2S_3')$
χ_5	E_g	$E(\epsilon)$	$(1/2)(Z_1 - Z_3 + Z_1' - Z_2')$
χ_6	E_g	$E(\epsilon)$	$(1/2)(S_1 - S_2 + S_1' - S_2')$
χ_7	T_{1g}	$E(x)$	$(1/24)^{1/2}(2X_1 + Y_1 - X_2 - 2Y_2 - X_3 + Y_3 + X_1' + 2Y_1' - 2X_2' - Y_2' + X_3' - Y_3')$
χ_8	T_{1g}	$E(y)$	$(1/8)^{1/2}(Y_1 + X_2 - X_3 - Y_3 + X_1' + Y_2' - X_3' - Y_3')$
χ_9	T_{1g}	$E(z)$	$(1/12)^{1/2}(X_1 - Y_1 + X_2 - Y_2 + X_3 - Y_3 - X_1' + Y_1' - X_2' + Y_2' - X_3' + Y_3')$
χ_{10}	T_{2g}	$E(\rho)$	$(1/24)^{1/2}(2X_1 - Y_1 - X_2 + 2Y_2 - X_3 - Y_3 - X_1' + 2Y_1' + 2X_2' - Y_2' - X_3' - Y_3')$
χ_{11}	T_{2g}	$E(\sigma)$	$-(1/8)^{1/2}(Y_1 - X_2 + X_3 - Y_3 + X_1' - Y_2' - X_3' + Y_3')$
χ_{12}	T_{2g}	A_1	$(1/12)^{1/2}(X_1 + Y_1 + X_2 + Y_2 + X_3 + Y_3 + X_1' + Y_1' + X_2' + Y_2' + X_3' + Y_3')$
χ_{13}	T_{1u}	$E(x)$	$-(1/12)^{1/2}(Z_1 + Z_2 - 2Z_3 - Z_1' - Z_2' + 2Z_3')$
χ_{14}	T_{1u}	$E(x)$	$-(1/12)^{1/2}(S_1 + S_2 - 2S_3 - S_1' - S_2' + 2S_3')$
χ_{15}	T_{1u}	$E(x)$	$-(1/24)^{1/2}(X_1 - 2Y_1 - 2X_2 + Y_2 + X_3 + Y_3 + 2X_1' - Y_1' - X_2' + 2Y_2' - X_3' - Y_3')$
χ_{16}	T_{1u}	$E(y)$	$(1/2)(Z_1 - Z_2 - Z_1' + Z_2')$
χ_{17}	T_{1u}	$E(y)$	$(1/2)(S_1 - S_2 - S_1' + S_2')$
χ_{18}	T_{1u}	$E(y)$	$-(1/8)^{1/2}(X_1 - Y_2 - X_3 + Y_3 - Y_1' + X_2' - X_3' + Y_3')$
χ_{19}	T_{1u}	A_2	$(1/6)^{1/2}(Z_1 + Z_2 + Z_3 - Z_1' - Z_2' - Z_3')$
χ_{20}	T_{1u}	A_2	$(1/6)^{1/2}(S_1 + S_2 + S_3 - S_1' - S_2' - S_3')$
χ_{21}	T_{1u}	A_2	$(1/12)^{1/2}(X_1 + Y_1 + X_2 + Y_2 + X_3 + Y_3 - X_1' - Y_1' - X_2' - Y_2' - X_3' - Y_3')$
χ_{22}	T_{2u}	$E(\theta)$	$-(1/24)^{1/2}(X_1 + 2Y_1 - 2X_2 - Y_2 + X_3 - Y_3 - 2X_1' - X_1' + X_2' + 2Y_2' + X_3' - Y_3')$
χ_{23}	T_{2u}	$E(\epsilon)$	$(1/8)^{1/2}(X_1 + Y_2 - X_3 - Y_3 - Y_1' - X_2' + X_3' + Y_3')$
χ_{24}	T_{2u}	A_1	$(1/12)^{1/2}(X_1 - Y_1 + X_2 - Y_2 + X_3 - Y_3 + X_1' - Y_1' + X_2' - Y_2' + X_3' - Y_3')$

[a] The 2s, $2p_x$, $2p_y$, and $2p_z$ atomic orbitals located at ligand site λ (=1, 2, 3, 1', 2', or 3') are denoted by S_λ, X_λ, Y_λ, and Z_λ, respectively.

Table III. Crystal Field Matrix Elements[a]

A. Diagonal Terms

$\langle 3d_{z^2}|V|3d_{z^2}\rangle = -Q\{6/R + (6/7R^3)(3\cos^2\theta - 1)\langle R_{3d}|r^2|R_{3d}\rangle + (3/14R^5)(35\cos^4\theta - 30\cos^2\theta + 3)\langle R_{3d}|r^4|R_{3d}\rangle\}$

$\langle 3d_{xz}|V|3d_{xz}\rangle = -Q\{6/R + (3/7R^3)(3\cos^2\theta - 1)\langle R_{3d}|r^2|R_{3d}\rangle - (1/7R^5)(35\cos^4\theta - 30\cos^2\theta + 3)\langle R_{3d}|r^4|R_{3d}\rangle\}$

$\langle 3d_{x^2-y^2}|V|3d_{x^2-y^2}\rangle = -Q\{6/R - (6/7R^3)(3\cos^2\theta - 1) \times \langle R_{3d}|r^2|R_{3d}\rangle + (1/28R^5)(35\cos^4\theta - 30\cos^2\theta + 3)\langle R_{3d}|r^4|R_{3d}\rangle\}$

$\langle 3d_{yz}|V|3d_{yz}\rangle = \langle 3d_{xz}|V|3d_{xz}\rangle$

$\langle 3d_{xy}|V|3d_{xy}\rangle = \langle 3d_{x^2-y^2}|V|3d_{x^2-y^2}\rangle$

$\langle 4s|V|4s\rangle = -Q6/R$

$\langle 4p_x|V|4p_x\rangle = \langle 4p_y|V|4p_y\rangle = -Q\{6/R - (3/5R^3)(3\cos^2\theta - 1) \times \langle R_{4p}|r^2|R_{4p}\rangle\}$

$\langle 4p_z|V|4p_z\rangle = -Q\{6/R + (6/5R^3)(3\cos^2\theta - 1)\langle R_{4p}|r^2|R_{4p}\rangle\}$

B. Off-Diagonal Terms

$\langle 3d_{xz}|V|3d_{x^2-y^2}\rangle = -Q\{(5/2R^5)\sin^3\theta\cos\theta\langle R_{3d}|r^4|R_{3d}\rangle\}$

$\langle 3d_{z^2}|V|4s\rangle = -Q\{(3/5^{1/2}R^4)(3\cos^2\theta - 1)\langle R_{3d}|r^2|R_{4s}\rangle\}$

$\langle 3d_{xy}|V|4p_y\rangle = Q\{(5/7)^{1/2}(3/4R^4)\sin^3\theta\langle R_{3d}|r^3|R_{4p}\rangle\sum_{i=1}^{6}\cos 3\phi_i\}$

$\langle 3d_{x^2-y^2}|V|4p_x\rangle = -\langle 3d_{xy}|V|4p_y\rangle$

[a] In atomic units. $\langle R_i|r^n|R_j\rangle$ is a radial integral (see Table IV).

[a] In atomic units. $\langle R_i|r^n|R_j\rangle$ is a radical integral (see Table IV). The variables R, θ, and ϕ refer to ligand positions with respect to the trigonal metal coordinate system (see Figure 3).

Table IV. Formulas for the One-Center Radial Integrals[a]

$\langle R_{ns}|r|R_{np}\rangle = [(2n+1)!/(2n)!(\zeta_{ns}+\zeta_{np})][4\zeta_{ns}\zeta_{np}/(\zeta_{ns}+\zeta_{np})^2]^{n+1/2}$

$\langle R_{4p}|r^2|R_{4p}\rangle = 22.5/\zeta_{4p}^2$

$\langle R_{3d}|r^n|R_{4s(4p)}\rangle^{b,c} = [(7+n)!/2^n(6!8!)^{1/2}][C_1(\zeta_1/\bar{\zeta}_1)^{n/2}(\zeta_4/\bar{\zeta}_1)^{9/2}/\bar{\zeta}_1^{n} + C_2(\zeta_2/\bar{\zeta}_2)^{7/2}(\zeta_4/\bar{\zeta}_2)^{9/2}/\bar{\zeta}_2^{n}]$

$\langle R_{3d}|r^n|R_{3d}\rangle^{b,d} = [(6+n)!/(6!2^n)][C_1^2/\zeta_1^{n} + C_2^2/\zeta_2^{n} + 2C_1C_2(\zeta_1\zeta_2/\bar{\zeta}^2)^{7/2}/\bar{\zeta}^{n}]$

[a] In atomic units. [b] $R_{3d} = C_1R_{3d}(\zeta_1) + C_2R_{3d}(\zeta_2)$. [c] $\bar{\zeta}_1 = (\zeta_1 + \zeta_{4s(4p)})/2$, $\bar{\zeta}_2 = (\zeta_2 + \zeta_{4s(4p)})/2$. [d] $\bar{\zeta} = (\zeta_1 + \zeta_2)/2$.

the lth molecular orbital (a virtual orbital) is given by

$$\Psi_{k\to l} = |\psi_1(1)\bar{\psi}_1(2)\ldots\psi_k(2k-1)\bar{\psi}_l(2k)\ldots\bar{\psi}_m(2m)| \quad (12)$$

A given excited-state wave function will be a linear combination of these Slater determinants

$$\Psi_a = \sum_{k,l} C^a{}_{k,l}\Psi_{k\to l} \quad (13)$$

In our calculations we consider only single electron excitations so that the ground-state wave function is simply Ψ_0.

In order to determine the coefficients $C^a{}_{k,l}$ we employ a configuration interaction scheme in which the requisite electron repulsion integrals over atomic orbitals are approximated by the CNDO method. Although this procedure is rather crude for determining energies, it does provide state wave functions of the correct symmetry which we need in calculating the state transition moments.

C. Transition Integrals. 1. Dipole Length Matrix Elements. For a transition from the ground state, Ψ_0, to an excited state, Ψ_a, the electric dipole transition moment along one of the cartesian axes is

$$\langle\Psi_a|\hat{\mu}|\Psi_0\rangle = e\sum_{k,l} C^a{}_{k,l}\langle\Psi_{k\to l}|\hat{\mathbf{q}}|\Psi_0\rangle \quad (14)$$

where $\hat{\mathbf{q}} = \mathbf{i}x + \mathbf{j}y + \mathbf{k}z$. The matrix elements in the above sum may be expressed in terms of atomic orbitals, ϕ_i, as

$$\langle\Psi_{k\to l}|\hat{\mathbf{q}}|\Psi_0\rangle = \sum_{i=1}^{N}\sum_{j=1}^{N} C^*{}_{il}C_{jk}\langle\phi_i|\hat{\mathbf{q}}|\phi_j\rangle \quad (15)$$

In our calculations we neglect the two-center transition integrals over atomic orbitals. Previous calculations have shown that the contribution made by the two-center terms to the total transition moment is small enough to leave our conclusions unchanged. The one-center electric dipole transition integrals are given in Table V. In evaluating these integrals we require values for the radial integrals: $\langle R_{3d}|r|R_{4p}\rangle$ and $\langle R_{ns}|r|R_{np}\rangle$, where $n = 2$, 3, or 4. These integrals are computed from the formulas in Table IV.

Table V. One-Center Electric Dipole Transition Integrals[a]

$\langle ns|\hat{\mu}_x|np_x\rangle = \langle ns|\hat{\mu}_y|np_y\rangle = \langle ns|\hat{\mu}_z|np_z\rangle = 3^{-1/2}\langle R_{ns}|r|R_{np}\rangle$

$\langle 3d_{z^2}|\hat{\mu}_x|4p_x\rangle = \langle 3d_{z^2}|\hat{\mu}_y|4p_y\rangle = -\langle 3d_{z^2}|\hat{\mu}_z|4p_z\rangle/2 = -15^{-1/2}\langle R_{3d}|r|R_{4p}\rangle$

$\langle 3d_{xz}|\hat{\mu}_x|4p_z\rangle = \langle 3d_{xz}|\hat{\mu}_z|4p_x\rangle = \langle 3d_{yz}|\hat{\mu}_y|4p_z\rangle = 5^{-1/2}\langle R_{3d}|r|R_{4p}\rangle$

$\langle 3d_{yz}|\hat{\mu}_z|4p_y\rangle = \langle 3d_{x^2-y^2}|\hat{\mu}_x|4p_x\rangle = -\langle 3d_{x^2-y^2}|\hat{\mu}_y|4p_y\rangle = 5^{-1/2}\langle R_{3d}|r|R_{4p}\rangle$

$\langle 3d_{xy}|\hat{\mu}_x|4p_y\rangle = \langle 3d_{xy}|\hat{\mu}_y|4p_x\rangle = 5^{-1/2}\langle R_{3d}|r|R_{4p}\rangle$

[a] In atomic units. Radial integrals given in Table IV.

Table VI. One-Center Angular Momentum Transition Integrals[a]

$\langle np_x|L_x|np_y\rangle = \langle np_y|L_x|np_z\rangle = \langle np_z|L_y|np_x\rangle = 1$

$\langle nd_{z^2}|L_x|nd_{yz}\rangle = -\langle nd_{z^2}|L_y|nd_{xz}\rangle = -(3^{1/2})$

$\langle nd_{xz}|L_x|nd_{xy}\rangle = \langle nd_{x^2-y^2}|L_x|nd_{yz}\rangle = \langle nd_{x^2-y^2}|L_y|nd_{xz}\rangle = -1$

$\langle nd_{xy}|L_y|nd_{yz}\rangle = \langle nd_{yz}|L_z|nd_{xz}\rangle = -1$

$\langle nd_{x^2-y^2}|L_z|nd_{xy}\rangle = 2$

$\langle ns|L_x|np_y\rangle = \langle np_x|L_y|ns\rangle = -Z_1W^{b,c}$

$\langle ns|L_x|np_z\rangle = \langle np_x|L_z|ns\rangle = Y_1W$

$\langle ns|L_y|np_z\rangle = \langle np_y|L_z|ns\rangle = -X_1W$

[a] In units of $-i\hbar$. [b] (X_1, Y_1, Z_1) is the position of ligand 1 with respect to the trigonal metal coordinate system. See Figure 3. [c] $W = \langle ns|\partial/\partial q|np_q\rangle = (\zeta_{ns}\zeta_{np})^{n+1/2}[(n+1)/n - \zeta_{np}/\bar{\zeta}]/3^{1/2}\bar{\zeta}^{2n}$, where $\bar{\zeta} = (\zeta_{ns} + \zeta_{np})/2$.

The ligand–ligand transition moments are projected onto the metal's coordinate system by means of the transformation matrices discussed earlier. The projected moments are subsequently used in evaluating the state transition moments *via* eq 14 and 15.

2. Angular Momentum Matrix Elements. The angular momentum matrix elements are treated in the same fashion as the dipole length matrix elements. The angular momentum about the q axis for a transition from the ground state, Ψ_0, to an excited state, Ψ_a, is given by

$$\langle\Psi_a|\hat{L}_q|\Psi_0\rangle = \sum_{k,l} C^a{}_{k,l}\sum_{i=1}^{N}\sum_{j=1}^{N} C^*{}_{il}C_{jk}\langle\phi_i|\hat{L}_q|\phi_j\rangle \quad (16)$$

where $q = x$, y, or z. The total angular momentum operator, in the units $-i\hbar$, is

$$\hat{\mathbf{L}} = \hat{\mathbf{r}}\times\hat{\Delta} = \mathbf{i}[y\frac{\partial}{\partial z} - z\frac{\partial}{\partial y}] + \mathbf{j}[z\frac{\partial}{\partial x} - x\frac{\partial}{\partial z}] + \mathbf{k}[x\frac{\partial}{\partial y} - y\frac{\partial}{\partial x}] = \mathbf{i}\hat{L}_x + \mathbf{j}\hat{L}_y + \mathbf{k}\hat{L}_z \quad (17)$$

Table VI contains the pertinent angular momentum integrals in terms of atomic orbitals.

As was done with the dipole length matrix elements, we retain only the single-center terms in our calculations. The contributions made by the ligands to the total angular momentum are projected onto the coordinate system for the metal atom. This is accomplished in two steps. First we construct a coordinate system on the ligand that is parallel to that on the metal and project the angular momentum operator about this new ligand system onto the coordinate system centered on the metal atom. The projected operators are

$$\hat{L}_x = \hat{L}_{x'} + Y_L\frac{\partial}{\partial z'} - Z_L\frac{\partial}{\partial y'}$$

$$\hat{L}_y = \hat{L}_{y'} + Z_L\frac{\partial}{\partial x'} - X_L\frac{\partial}{\partial z'}$$

$$\hat{L}_z = \hat{L}_{z'} + X_L\frac{\partial}{\partial y'} - Y_L\frac{\partial}{\partial x'} \quad (18)$$

Table VII. Computational Parameters

			CoO_6	CoN_6	CrO_6	CrN_6
Metal	3d[a]	C_1	0.5980	0.5980	0.5460	0.5460
		C_2	0.5260	0.5260	0.5821	0.5821
		ζ_1	5.50	5.50	4.95	4.95
		ζ_2	2.50	2.50	2.20	2.20
	4s[b]	ζ	1.60	1.60	1.30	1.30
	4p[b]	ζ	1.45	1.45	1.48	1.48
Ligand	2s[c]	ζ	2.2458	1.9237	2.2458	1.9237
	2p[c]	ζ	2.2266	1.917	2.2266	1.917
R,[d] Å			1.925[e]	2.000[f]	1.960[g]	2.075[h]
F_σ[i]			1.70	1.60	1.70	1.60
Q_L			−0.3	0.0	−0.4	0.0

[a] $R'_{3d} = C_1R_{3d}(\zeta_1) + C_2R_{3d}(\zeta_2)$.[66a] [b] Reference 66b. [c] Reference 67. [d] Metal–ligand bond distance. [e] Reference 47. [f] Reference 49. [g] Reference 68. [h] Reference 69. [i] Reference 64.

where $\hat{L}_q$ is the projected operator, $\hat{L}_{q'}$ is the angular momentum about the q' axis located on the ligand, and parallel to the metal q axis, and (X_L, Y_L, Z_L) is the ligand position with respect to the metal atom's coordinate system. The effect of projecting the angular momentum operator is to give rise to nonzero angular momentum contributions from ligand s with ligand p orbitals. These additional matrix elements are also given in Table VI. The second step consists of transforming from the parallel coordinate system on the ligand to the original ligand coordinate ligand system (*i.e.*, the one about which the ligand atomic orbitals are quantized). This transformation is accomplished by the matrix method discussed earlier. Thus all of the angular momentum matrix elements appearing in the right-hand side of eq 16 are calculated with the metal atom at the origin.

D. Rotatory Strengths. The rotatory strength for a transition from the ground state, Ψ_0, to an excited state, Ψ_a, is given by

$$R_{0\to a} = \mathrm{Im}[\langle\Psi_0|\hat{\mu}|\Psi_a\rangle\cdot\langle\Psi_a|\hat{\mathbf{m}}|\Psi_0\rangle] \tag{19}$$

where Im means that the imaginary part of the expression is taken. The electric and magnetic dipole moment operators are defined respectively as

$$\hat{\mu} = e\sum_j \hat{\mathbf{r}}_j \tag{20}$$

and

$$\hat{\mathbf{m}} = -i(\hbar e/2mc)\sum_j \hat{\mathbf{r}}_j \times \hat{\Delta}_j \tag{21}$$

where the sums extend over all electrons. Typical magnitudes of R for the d–d transitions in dissymmetric metal complexes are $\sim 10^{-40}$ cgsu. Instead of dealing with such small numbers, we shall find it convenient to report our results in terms of *reduced rotatory strengths*. The reduced rotatory strength of a transition $0 \to a$ is defined as

$$[R_{0\to a}] = (100/\beta D)\,\mathrm{Im}[\langle\Psi_0|\hat{\mu}|\Psi_a\rangle\cdot\langle\Psi_a|\hat{\mathbf{m}}|\Psi_0\rangle] \cong 1.08 \times 10^{40} R_{0\to a}(\mathrm{cgsu}) \tag{22}$$

where β is the Bohr magneton and D is the Debye unit (10^{-18} esu cm).

E. Structure Variables and Computational Parameters. In Table VII are listed the computational parameters and metal–ligand bond distances employed in the present study for various complex ions.[47,49,64,66-69] Metal–ligand bond distance is held constant for all calculations carried out on a particular ML_6 cluster. The distortion angles, δ and σ, are treated as independent variables and the reduced rotatory strength and trigonal splitting energy are the dependent variables in the calculations. The results reported in this paper were obtained with just one set of W–H parameters, F_σ, F_π, F_1, for each complex ion studied. Although a thorough sensitivity analysis was not performed, the dependent variables of this study were not sensitive to 20–30% changes in the W–H parameters. Furthermore, they were insensitive to ligand charge parameters, Q_L, over a range of values considered reasonable for these quantities. Only one set of VOIP were calculated[58] and only one set of radial functions were used for both the metal[66] and the ligand[67] basis orbitals. Although the absolute magnitudes of the

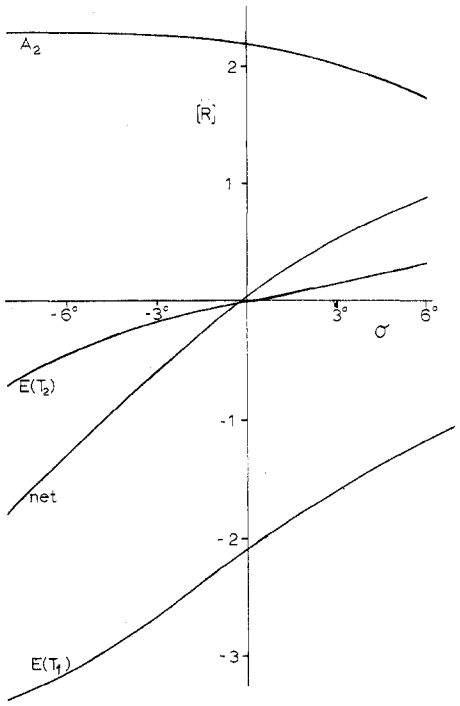

Figure 4. $[R]$ *vs.* σ at $\delta = 3°$ for $Co^{III}O_6$; net value of $[R]$ and component values of $[R]$.

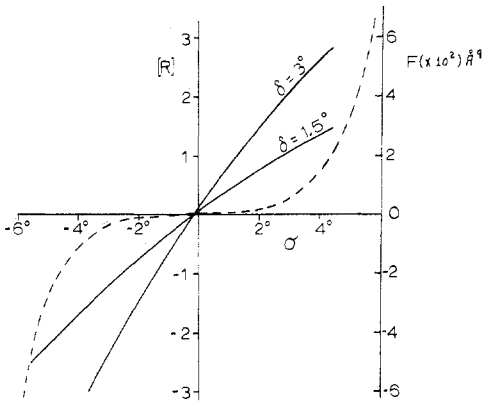

Figure 5. $[R]$ *vs.* σ for $\delta = 3$ and 1.5° for $Co^{III}O_6$; net value of $[R]$ (solid lines). F *vs.* σ for $\delta = 3°$ (broken line). $F = -X_LY_LZ_L\cdot(X_L^2 - Y_L^2)(Y_L^2 - Z_L^2)(Z_L^2 - X_L^2)$; (X_L, Y_L, Z_L) = cartesian positional coordinates of ligating atoms (O) referred to cubic coordinate system of Figure 2.

(66) (a) J. W. Richardson, W. C. Nieuwpoort, R. R. Powell, and W. F. Edgell, *J. Chem. Phys.*, 36, 1057 (1962); (b) J. W. Richardson, R. R. Powell, and W. C. Nieuwpoort, *ibid.*, 38, 796 (1963).

(67) E. Clementi and D. L. Raimondi, *J. Chem. Phys.*, 38, 3686 (1963).

(68) J. N. van Niekerk and F. R. L. Schoening, *Acta Crystallogr.*, 5, 499 (1952).

(69) K. N. Raymond, P. W. R. Corfield, and J. A. Ibers, *Inorg. Chem.*, 7, 1362 (1968).

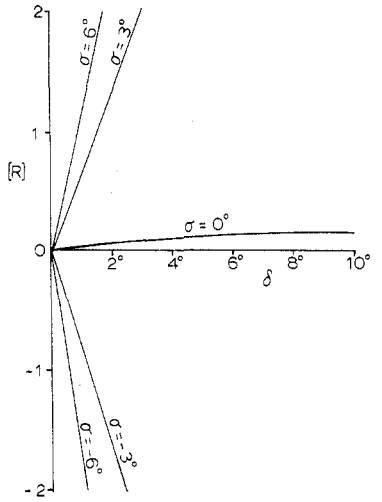

Figure 6. $[R]$ *vs.* δ for $\sigma = 3$, 0, and $-6°$ for $Co^{III}O_6$; net value of $[R]$.

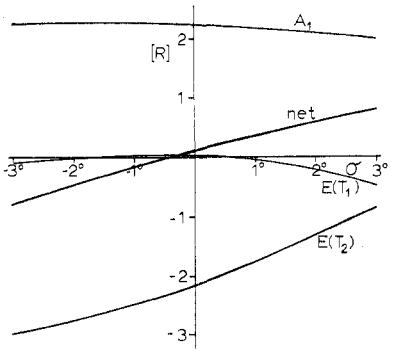

Figure 7. $[R]$ *vs.* σ at $\delta = 3°$ for $Cr^{III}O_6$; net value of $[R]$ and component values of $[R]$.

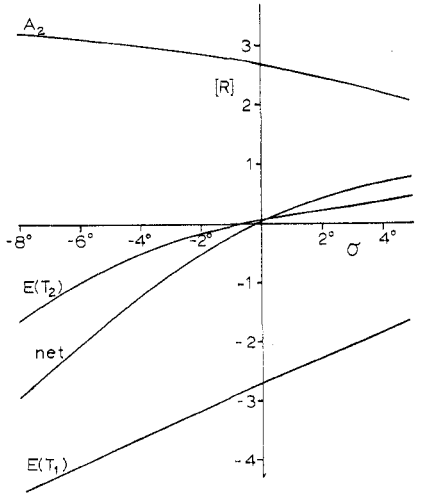

Figure 8. $[R]$ *vs.* σ at $\delta = 3°$ for $Co^{III}N_6$, σ and π bonding; net value of $[R]$ and component values of $[R]$.

computed rotatory strengths most certainly are sensitive to these computational parameters, it is doubtful that the qualitative and semiquantitative relationships between rotatory strength and the chiral distortion variables will be fundamentally altered.

III. Results

The principal results of this study are presented in Figures 4–11. In Figures 4–8, the reduced rotatory strengths computed on our extended version of Piper's model are plotted

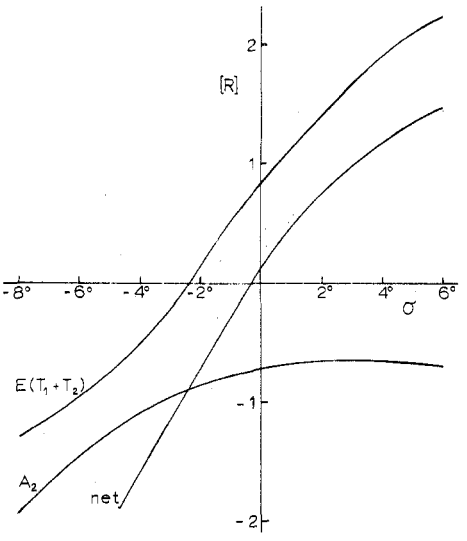

Figure 9. $[R]$ *vs.* σ at $\delta = 3°$ for $Co^{III}N_6$, π bonding suppressed; net value of $[R]$ and component values of $[R]$.

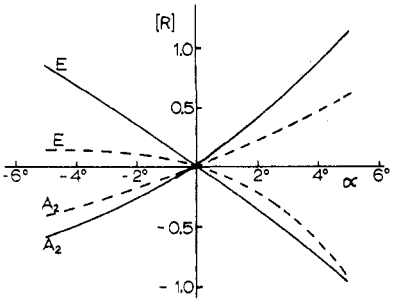

Figure 10. $[R]$ *vs.* α at $\sigma = 0°$ and $\delta = 0°$ for $Co^{III}N_6$, canted ligand orbitals. For "ob" isomer, $\lambda = 30°$ (Λ configuration). For "lel" isomer, $\lambda = 60°$ (Λ configuration).

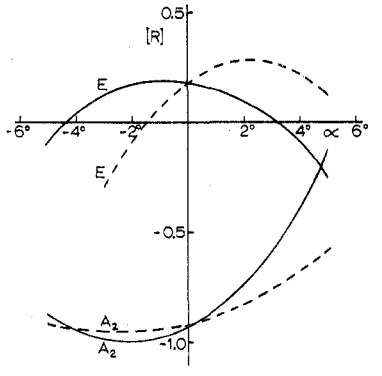

Figure 11. $[R]$ *vs.* α at $\sigma = -2°$ and $\delta = 3°$ for $Co^{III}N_6$, trigonally displaced ligands and canted ligand orbitals. For "ob" isomer, $\lambda = 30°$ (Λ configuration). For "lel" isomer, $\lambda = 60°$ (Λ configuration).

against one of the trigonal distortion coordinates, either σ or δ. Recall that $\sigma < 0°$ ($\sigma > 0°$) corresponds to a ML_6 cluster compressed (elongated) along a trigonal (C_3) axis. Only positive values of δ appear in any of the figures since, of course, the magnitude of $[R]$ depends only upon the magnitude of δ for any given value of σ. That is, a change in sign of δ results only in a change of sign of $[R]$, not a change in magnitude. Moreover, the rotatory strengths are found to be linearly related to the azimuthal distortion (Figures 5, 6) for values of $|\delta| < \sim 6°$, so that we need only present results for a single value of δ. The dependence of $[R]$ upon both the sign and the magnitude of σ is somewhat

more subtle, and both positive and negative values of σ are represented in the figures.

In Figure 9 are presented reduced rotatory strengths calculated on Piper's original model *vs.* σ for a $Co^{III}N_6$ cluster. Figure 10 contains similar results calculated on Liehr's molecular orbital model. As stated earlier, Liehr's model allows for precessing of the ligand p_σ orbital about the metal–ligand internuclear axis and in Figure 10 we have tailored the model to correspond to the "lel" and "ob" conformers of Λ-$Co(en)_3^{3+}$. Combining Piper's and Liehr's models leads to the results depicted in Figure 11. Again these results are designed to correspond to the "lel" and "ob" conformers of Λ-$Co(en)_3^{3+}$.

The net rotatory strength for a given structure is just the algebraic sum of all one-electron d–d rotatory strengths. Each of our chiral Co(III) species has trigonal dihedral (D_3) symmetry so that only three nonvanishing component rotatory strengths are calculated. These correspond to the transitions $^1A_1(A_1) \rightarrow {}^1A_2(T_1)$, $^1A_1(A_1) \rightarrow {}^1E(T_1)$, and $^1A_1(A_1) \rightarrow {}^1E(T_2)$, where the symbols in parentheses refer to the octahedral parent states (with parity and spin multiplicity suppressed). The trigonal transition, $^1A_1(A_1) \rightarrow {}^1A_1(T_2)$, is forbidden in both magnetic dipole and electric dipole radiation and is, therefore, optically inactive. Each of our chiral Cr(III) species has trigonal dihedral (D_3) symmetry so, again, only three nonvanishing component rotatory strengths are calculated. These correspond to the following spin-allowed transitions: $^4A_2(A_2) \rightarrow {}^4A_1(T_2)$, $^4A_2(A_2) \rightarrow {}^4E(T_2)$, and $^4A_2(A_2) \rightarrow {}^4E(T_1)$.

In all of our calculations on $Co^{III}O_6$ and on $Cr^{III}O_6$ we included both σ- and π-bonding interactions between metal and ligand. Furthermore, we assumed isotropic π bonding insofar as the local $2p_x$ and $2p_y$ ligand atomic orbitals were treated identically. In a real system such as tris(oxalato)-cobalt(III) one might expect some anisotropy among the ligand π-bonding orbitals in the plane perpendicular to the metal–ligand internuclear axis due to the influence of chelate ring atoms. On our model, these possible anisotropies are neglected. We performed four sets of calculations on the $Co^{III}N_6$ species. In one set both σ- and π-bonding interactions were included while in another set π bonding was suppressed by restricting the ligand atomic orbital basis to 2s and $2p_z$ functions. From a comparison of the results displayed in Figures 8 and 9, it is readily apparent that π bonding between the metal ion and the ligator atoms has a pronounced influence on the d–d rotatory strengths. The remaining sets of calculations on the $Co^{III}N_6$ cluster involve a canted p_σ orbital on each ligator atom. As shown in section II, the canted p_σ orbital may be decomposed into σ- and π-bonding p orbitals. Nevertheless we consider these calculations to correspond to a σ-bonding complex since there is only one ligator atom p orbital available for bonding. Canting of the p_σ orbital is included to simulate the directional effects of the nonligating atoms on the ligand p_σ orbital.

The trigonal field splitting energies calculated as a function of distortion angle σ are plotted in Figure 12 for $Co^{III}O_6$, $Cr^{III}O_6$, and $Co^{III}N_6$ (π bonding suppressed) at a constant value of $\delta = 3°$. In Figure 13, the trigonal field splitting energy in $Co^{III}O_6$, $\sigma = 0°$, is plotted *vs.* the distortion angle δ. If the doubly degenerate trigonal component is of lower energy than the nondegenerate trigonal component, the trigonal splitting energy, ν, is positive. That is $\nu\ (cm^{-1}) = [\epsilon(a) - \epsilon(e)]/hc$, where $\epsilon(a)$ and $\epsilon(e)$ are the computed energies of the nondegenerate and degenerate trigonal components, respectively.

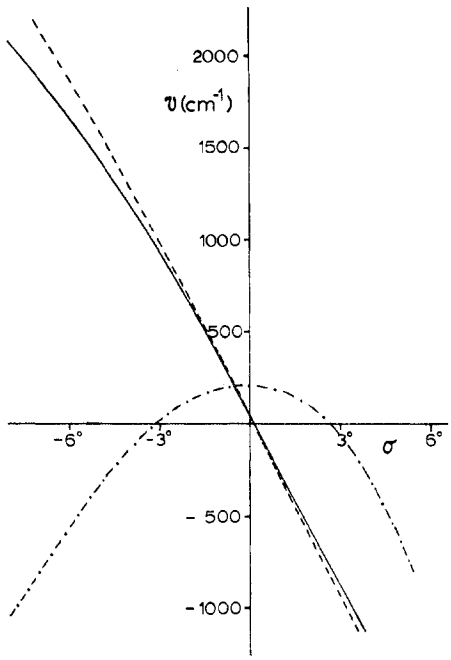

Figure 12. Trigonal field splitting energy, ν (cm^{-1}), *vs.* σ: $Co^{III}O_6$, $\delta = 3°$, ————; $Cr^{III}O_6$, $\delta = 3°$, - - - - - - - - - - - -; $Co^{III}N_6$, $\delta = 3°$, π bonding suppressed, ·—— ·—— ·——.

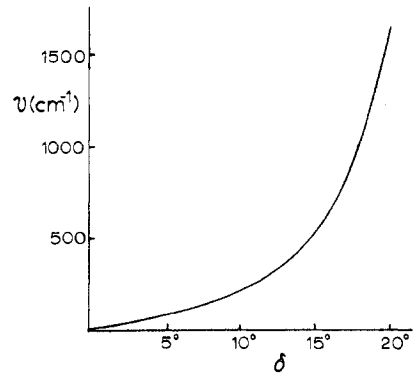

Figure 13. Trigonal field splitting energy, ν (cm^{-1}), *vs.* δ for $Co^{III}O_6$ at $\sigma = 0°$.

IV. Discussion

The linear dependence of net d–d rotatory strengths on the degree of twist about the trigonal axis of ML_6 clusters is a consequence of the model adopted in this study. Similar behavior is found for the trigonal components of the d–d transitions in trigonally distorted CoO_6, CrO_6, CoN_6, and CrN_6. Even if the ligand p_π orbitals are excluded (Piper's model), this behavior still obtains. For this reason we need present calculations for only a single value of δ in the linear region since the properties of structures with different degrees of azimuthal distortion can be obtained by interpolation or extrapolation.

From a comparison of Figures 4, 7, and 8 with Figure 9 it is readily apparent that π bonding between the metal ion and the ligator atoms has a pronounced influence on the d–d rotatory strengths. The most striking feature is that the signs of the rotatory strengths of the lowest energy d–d transitions change upon inclusion of the ligand p_π orbitals for $\sigma > -3°$. Karipedes and Piper[30] suggested that π-bonding contributions to the electric dipole transition moments would be opposite in sign to those expected of the σ-bond contributions for d–d transitions, but they

further argued that the π-bonding contributions could be neglected for $Co(en)_3^{3+}$.

With regard to $Co(en)_3^{3+}$, the reduced rotatory strengths calculated for the d-d transitions on Piper's model do not agree in relative magnitude with those obtained from the experimental CD spectra. In crystalline form the CoN_6 cluster of $Co(en)_3^{3+}$ suffers an azimuthal contraction and a polar compression.[50] It may be conjectured that in solution the polar distortion in $Co(en)_3^{3+}$ is relaxed with the result that the ratio of the E to A_2 rotatory strengths increases (Figure 9). Woldbye[10] and Mason[32,70] have argued that the shape of the solution CD spectrum of $Co(en)_3^{3+}$ may be interpreted on the basis of an equilibrium mixture of isomeric structures formed by the various combinations of chelate ring λ and δ conformers. This argument rests on the assumption that the chiroptical properties of the ($\delta\delta\delta$), ($\delta\delta\lambda$), ($\delta\lambda\lambda$), and ($\lambda\lambda\lambda$) structures of a given configurational isomer (Δ or Λ) are sufficiently different that the experimental CD spectra will be sensitive to their relative concentrations in solution.

Unless the positions of the ligator atoms are altered on going from one chelate ring conformer to another, Piper's model predicts that the d-d rotatory strengths will be insensitive to chelate ring conformation. Liehr's model leads to an opposite prediction. Referring to Figure 10 we see that for a negative angle of cant Liehr's model predicts a positive $E(T_{1g})$ CD band and a negative $A_2(T_{1g})$ CD band for complexes with the Λ configuration. On going from the "lel" ($\delta\delta\delta$) to the "ob" ($\lambda\lambda\lambda$) structure Liehr's model predicts a much greater reduction in the $E(T_{1g})$ rotatory strength than in the $A_2(T_{1g})$ rotatory strength. However, the "lel" and "ob" structures both give the same sign for the d-d rotatory strengths for all values of α considered. That is, R(E) for the "lel" structure has the same sign as R(E) for the "ob" structure and likewise for the R(A) values. These results are contrary to Woldbye's suggestion that the positive and negative bands observed in the CD spectrum of Λ-$Co(en)_3^{3+}$ between 500 and 400 nm are attributable to "lel" and "ob" isomers rather than to the E and A trigonal components of the $A_{1g} \rightarrow T_{1g}$ transition.

If the ligator atoms are displaced from their octahedral positions and their donor orbitals are canted with respect to the metal-ligand internuclear axes, then the salient features of both Piper's and Liehr's models are represented. The results displayed in Figure 11 were calculated for CoN_6 structures in which the geometry of the CoN_6 cluster approximates that found in the crystal structure of $2Co(en)_3Cl_3$, NaCl, and $6H_2O$,[71] and the angle of cant α was varied from -5 to $+5°$. Since the experimentally determined C-N-Co angle in $Co(en)_3^{3+}$ is very nearly tetrahedral, any reasonable guess at what α should be certainly would be within the range $5° > \alpha > -5°$. As was the case for the pure Liehr model (undisplaced ligator atoms, but $\alpha \neq 0°$), the change in magnitude of the R(E) value on going from "lel" to "ob" outweighs the corresponding change in magnitude of R(A) for small values of α. Thus, on the model calculations presented here, an equilibrium mixture of "lel" and "ob" isomers cannot account for the sign and intensity pattern found in the CD spectrum of $Co(en)_3^{3+}$.

The results in Figures 9-11 indicate the sensitivity of the d-d rotatory strengths to the orientation of the ligand p_σ orbitals. A negative angle of cant in Liehr's model positions the ligand p_σ orbitals in the vicinity of the p_σ orbitals in Piper's model for an azimuthal contraction. Such positioning determines the sign of the d-d rotatory strengths while the precise orientation determines the magnitudes. If it is assumed that crystal forces are responsible for the polar compression observed for $Co(en)_3^{3+}$ in crystalline media and that in solution the complex is polar elongated, then the ratio of the calculated E and A rotatory strengths approaches that found in the experimental CD spectrum of that species. Relaxation of the polar compression should also result in a larger azimuthal contraction which would increase the magnitudes of the d-d rotatory strengths.

The CD spectra of tris(diamine)cobalt(III) complexes containing substituents on the ligand "backbone" have been analyzed in terms of vicinal and configurational effects with some success. In view of the calculated sensitivity of the rotatory strengths to the precise orientation of the ligand p_σ orbitals such analyses should be applied with caution. The CD spectra of Λ-$Co(en)_3^{3+}$ and Λ-$Co(d\text{-pn})_3^{3+}$ are quite similar,[9] but a marked change is observed in the CD spectrum of Λ-$Co(d\text{-cptn})_3^{3+}$, where cptn = *trans*-1,2-diaminocyclopentane.[72] The bands are shifted to lower energy in this latter species compared to Λ-$Co(en)_3^{3+}$ and the ratio of intensities of the E and A CD bands is inverted from that in Λ-$Co(en)_3^{3+}$. It is difficult to rationalize these spectral changes in terms of additive vicinal and configurational effects. On Piper's model the solution CD spectrum of Λ-$Co(en)_3^{3+}$ may be interpreted in terms of a polar elongation and azimuthal contraction of the CoN_6 cluster from the octahedral geometry. The addition of a methyl group to the carbon backbone would tend to reduce the elongation through steric effects and thereby decrease the ratio of the E to A rotatory strengths. In Λ-$Co(d\text{-cptn})_3^{3+}$ the CoN_6 cluster must suffer a polar compression with a resulting further decrease in the ratio of the E to A CD bands.

The "lel" isomer of Λ-$Co(d\text{-pn})_3^{3+}$ exhibits two CD bands of opposite signs in the 500-400-nm spectral region while the "ob" isomer of Δ-$Co(d\text{-pn})_3^{3+}$ exhibits only one band.[32,73] Apparently the trigonal splitting is very small for the "ob" isomer and the A CD band is masked by the E band. Additionally, the intensities of the d-d CD bands of $Co(pn)_3^{3+}$ are similar to those observed for $Co(en)_3^{3+}$. We interpret these results to mean that the azimuthal distortion in $Co(pn)_3^{3+}$ is similar to that in $Co(en)_3^{3+}$ and that there is an increase in the polar elongation of $Co(pn)_3^{3+}$ on going from the "lel" form to the "ob" form.

In several previous theoretical and experimental studies on the optical activity associated with the d-d transitions of six-coordinate Co(III) complexes, it has been asserted that the sign of the $E(T_{1g})$ CD band can be correlated with the stereochemical features of the ligand structure through use of the octahedral sector or regional rule.[32,42] According to this rule, the sign of the $A_1 \rightarrow E(T_{1g})$ rotatory strength in trigonal dihedral complexes is gauged by the sign of the function $F = -\Sigma_p X_p Y_p Z_p (X_p^2 - Y_p^2)(Y_p^2 - Z_p^2)(Z_p^2 - X_p^2)$, where (X_p, Y_p, Z_p) are the cartesian positional coordinates of the pth ligand perturbing atom and the summation extends over all perturbing atoms in the ligand environment. This rule has its basis in the one-electron theory of optical activity and in the crystal field model for the d-d excitations of transition metal complexes. If to zeroth order the six-coordinate metal complex is assumed to pos-

(70) A. J. McCaffery, S. F. Mason, and B. J. Norman, *Chem. Commun.*, 49 (1965).
(71) K. Nakatsu, M. Shiro, Y. Saito, and H. Kuroya, *Bull. Chem. Soc. Jap.*, 30, 158 (1957).
(72) M. Ito, F. Marumo, and Y. Saito, *Inorg. Nucl. Chem. Lett.*, 6, 519 (1970).
(73) K. Ogino, K. Murano, and J. Fujita, *Inorg. Nucl. Chem. Lett.*, 4, 351 (1968).

sess octahedral symmetry (O_h), then the complex can gain optical activity to first order on a crystal field perturbation expansion only if the perturbing field transforms as a pseudoscalar function under the symmetry operations of the O_h point group (*i.e.*, the perturbation must transform as the A_{1u} irreducible representation of O_h). If the crystal field potential is expanded in spherical harmonic functions about the metal ion, the first term that transforms as A_{1u} is of degree nine ($l = 9$), and that part of the potential function which depends upon perturber positions is just the function F, as defined above (actually FR_p^{-19}, where R_p is the metal-perturber radial distance).

In most applications of the "octahedral sector rule," primary emphasis has been placed on the nonligating atoms of the ligand environment as perturber centers. However, in a recent study of chiral Co(III) complexes Bosnich[42] has also attempted to include distortions of the CoL_6 cluster in a structure-spectra analysis based on the octahedral sector rule. In this latter application the dissymmetrically disposed ligating atoms are treated as perturbers and each makes a contribution to the function F. The theoretical validity of the octahedral sector rule, as well as its reliability in making spectra-structure correlations, has been discussed recently by Richardson[41] and will not be further examined here. However, we did calculate F as a function of polar distortion angle σ for several values of the azimuthal distortion angle δ and found that the signs of F for $|\sigma| \leq 10°$, $|\delta| \leq 10°$ were identical with the signs of the net reduced rotatory strengths calculated for CoO_6. In Figure 5, F is plotted *vs.* σ for $\delta = 3°$. Note that although F and $[R]$ have the same signs in this plot for $|\sigma| \leq 4°$, the shapes of the $[R]$ and F curves are somewhat different.

V. Summary

Although there has been a great deal of spectra-structure rationalization based on Liehr's and Piper's molecular orbital models for d-d optical activity, virtually no model calculations have been reported in the literature. Our calculations support the contention that trigonal dihedral transition metal complexes gain substantial optical activity in the visible region by the dissymmetric positioning of the ligating atoms. However, we must conclude that the effect of the nonligating atoms need be included in some fashion if the relative intensities of the visible CD bands are to be accurately calculated and accounted for. These intensities are expected to be sensitive to the computational model for the molecular orbitals, but the signs of the bands appear insensitive to changes in the parameters of the MO model. It is this latter quality, the ability of Piper's model correctly to predict signs of the CD bands, that is its greatest strength.

The extension of Piper's model to include ligand p_π atomic orbitals leads to overestimates of the amount of π bonding. It is possible that this defect may be remedied by including nonligating atoms bonded to the ligator atoms. That is, some anisotropy must be introduced into the ligand-metal π system to reflect the presence of the chelate bridging atoms.

Registry No. Cobalt, 7440-48-4; chromium, 7440-47-3.

Acknowledgments. We express our gratitude to the donors of the Petroleum Research Fund, administered by the American Chemical Society, for financial support of this research. We also acknowledge several helpful discussions with Dr. Warren Yeakel concerning the molecular orbital calculations reported here.

Contribution from the Department of Chemistry, DePauw University, Greencastle, Indiana 46135

Rates of Acid Hydrolysis and Stabilities of Ruthenium(II) Pentaammine Chloride and Bromide Complex Ions

GEOFFREY N. COLEMAN, JAMES W. GESLER, FRANK A. SHIRLEY, and JOHN R. KUEMPEL*[1]

Received August 22, 1972

A cyclic voltammetric method has been used to study the acid hydrolysis reactions $Ru(NH_3)_5X^+ + H_2O \rightarrow Ru(NH_3)_5H_2O^{2+} + X^-$, where X^- is Cl^- and Br^-. First-order rate constants, k, were measured in *p*-toluenesulfonic acid media over a temperature range of 15–40°. For the Cl^- complex, $k = 6.3 \pm 0.3$ sec^{-1} at 25°, $\Delta H^\ddagger = 12 \pm 3$ kcal, $\Delta S^\ddagger = -16 \pm 6$ eu; for the Br^- complex, $k = 5.4 \pm 0.4$ sec^{-1} at 25°, $\Delta H^\ddagger = 14 \pm 3$ kcal, $\Delta S^\ddagger = -10 \pm 6$ eu. Equilibrium constants for the reactions are found to be 0.70 *M* for the Cl^- hydrolysis and 0.92 *M* for the Br^- hydrolysis.

Introduction

Ruthenium(II) pentaammine complexes containing a sixth ligand which is not a π acceptor are difficult to isolate in aqueous solution. Several workers[2-4] have reported that these complexes undergo hydrolysis reactions very quickly after being produced by the reduction of corresponding ruthenium(III) pentaammine complexes. We have been attempting fast electrochemical reductions of ruthenium(III) complexes of this type to produce and observe the reduced complexes before they react. The objectives of the work were to measure hydrolysis rates and stabilities of these labile complexes for comparison with those of previously studied d^6 metal-ammine complexes.

Experimental Section

Reagents. $[Ru(NH_3)_5Cl]Cl_2$ and $[Ru(NH_3)_5Br]Br_2$ were prepared from $RuCl_3$ (Fischer Scientific) as described in the literature.[5] Uv spectra of aqueous solutions containing known amounts of these

(1) Address correspondence to this author at the Division of Science and Mathematics, Eisenhower College, Seneca Falls, N. Y. 13148.

(2) J. F. Endicott and H. Taube, *Inorg. Chem.*, 4, 437 (1965).

(3) J. H. Baxendale, R. A. Rodgers, and N. D. Ward, *J. Chem. Soc. A*, 1246 (1970).

(4) H. S. Lim, D. J. Barclay, and F. C. Anson, *Inorg. Chem.*, 11, 1460 (1972).

(5) A. D. Allen, F. Bottomley, R. O. Harris, V. P. Reinsalu, and C. V. Senoff, *Inorg. Syn.*, 12, 2 (1970).